Supporting information

Electrical Doping Effect of Vacancies in Monolayer MoS_2

Jing Yang,[†*] Hiroyo Kawai,[†] Calvin Pei Yu Wong[†] and Kuan Eng Johnson Goh[†,‡*]

[†]*Institute of Materials Research and Engineering, A*STAR (Agency for Science, Technology and Research), 2 Fusionopolis Way, Innovis, #08-03, 138634 Singapore*

[‡]*Department of Physics, Faculty of Science, National University of Singapore, 2 Science Drive 3, 117551 Singapore*

*Corresponding Authors' Emails: yangjing@imre.a-star.edu.sg; kejgoh@yahoo.com; gohj@imre.a-star.edu.sg

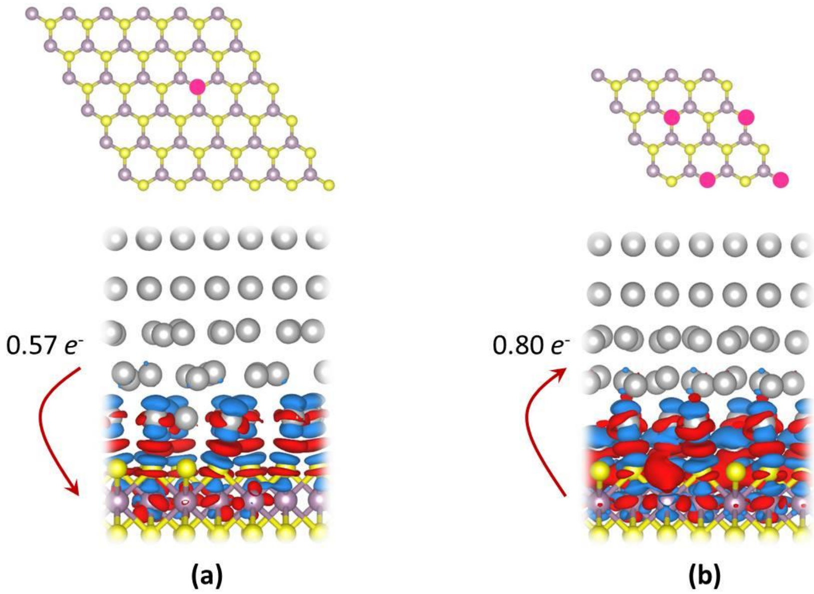

Figure S1: Top view of (a) V_{1S} within a 6×6 unit cell and (b) evenly distributed V_{4S} within a 4×4 unit cell, with the electron density difference map associated with the interaction between Au and MoS_2 with each V_S configuration shown directly below. Blue and red zones correspond to electron reduction and accumulation areas, respectively. Grey, yellow and purple spheres represent Au, S, Mo and atoms. The pink dots represent the V_S position. The arrow and the number show the charge transfer direction and amount predicted by Bader charge. Note the different configuration here results in the degree of charge transfer in (b) being lower than that for Fig. 1(e) and Fig. 5(e), despite having the same V_s density.

Table S1. Charge transfer amount (per surface Au atom, in e^-) calculated with different K-points mesh. A positive charge transfer amount corresponds to the charge flow from MoS_2 to Au, suggesting an *n*-type contact, and a negative charge transfer denotes an opposite direction, indicating a *p*-type contact.

vacancy type	2×2×1	4×4×1	6×6×1
1S	-0.018	-0.021	-0.022
4S	0.062	0.056	0.055

Table S2. Charge transfer amount (total and per surface Au atom, in e^-) calculated for different vacancy types. A positive charge transfer amount corresponds to the charge flow from MoS_2 to Au, suggesting an *n*-type contact, and a negative charge transfer denotes an opposite direction, indicating a *p*-type contact.

systems	charge transfer amount (in e^-)	
	total	per surface Au atom
pristine	-0.060	~0.00
V_{1S} (6×6 unit cell)	-0.57	-0.016
V_{1S}	0.28	-0.018
V_{2S}	0.31	0.019
V_{3S}	0.72	0.045
V_{4S}	0.99	0.062
V_{4S} (evenly distributed)	0.80	0.050
V_{1Mo}	-0.52	-0.033
V_{2Mo}	-0.56	-0.035

I-V curve simulation: In the main text, we simulated the junction current of Au-MoS_2 contact using the Schottky-Mott model and the thermionic emission model. Here, we explain these models in more details and explain how we obtain the simulated curves.

By the Schottky-Mott model, the pristine *n*-type Schottky barrier height $\phi_{b,n}$ is given by:

$$\phi_{b,n} = \Phi_M - \chi_S = 1 \text{ eV}$$

where Φ_M is the metal work function of Au (~ 5.1 eV) and χ_S is the electron affinity of MoS_2 (~ 4.1 eV).

The *p*-type Schottky barrier height $\phi_{b,p}$ can be estimated using the band gap of monolayer MoS_2 (1.8 eV).

$$\phi_{b,p} = E_g - \phi_{b,n} = 0.8 \text{ eV}$$

For simulating the junction current, we used the thermionic emission model which is given by:

$$J = \left[A^{**}T^2 \exp\left(\frac{-q\phi_b}{kT}\right)\right]\left[\exp\left(\frac{q(V - IR_S)}{nkT}\right) - 1\right]$$

where *J* (Acm^{-2}) is the current density of the device , *A*** is the effective Richardson constant of MoS_2 (= 44.8 $Acm^{-2}K^{-1}$), *q* is the electronic charge (= 1.602×10^{-19} C), *T* (K) is the absolute temperature, *k* is the Boltzmann constant (= 8.617×10^{-5} eVK^{-1}) , ideality factor *n* = 1 (ideal diode), R_s is the series resistance (assumed to be 25 Ω).

Complete references for those with more than 10 authors:

16. Kim, I. S.; Sangwan, V. K.; Jariwala, D.; Wood, J. D.; Park, S.; Chen, K. S.; Shi, F.; Ruiz-Zepeda, F.; Ponce, A.; Jose-Yacaman, M.; Dravid, V. P.; Marks, T. J.; Hersam, M. C.; Lauhon, L. J. Influence of Stoichiometry on the Optical and Electrical Properties of Chemical Vapor Deposition Derived MoS_2. *ACS Nano* **2014**, *8*, 10551- 10558.

17. Qiu, H.; Xu, T.; Wang, Z.; Ren, W.; Nan, H.; Ni, Z.; Chen, Q.; Yuan, S.; Miao, F.; Song, F.; Long, G.; Shi, Y.; Sun, L. Wang, J. Wang, X. Hopping Transport through Defect-Induced Localized States in Molybdenum Disulphide. *Nat. Comm.* **2013**, *4*, 2642.

20. Qiu, H.; Xu, T.; Wang, Z.; Ren, W.; Nan, H.; Ni, Z.; Chen, Q.; Yuan, S.; Miao, F.; Song, F.; Long, G.; Shi, Y.; Sun, L.; Wang, J.; Wang, X. All the Catalytic Active Sites of MoS_2 for Hydrogen Evolution. *J. Am. Chem. Soc.* **2016**, *138*, 16632-16638.

27. S. Ida, K. Sato, T. Nagata, H. Hagiwara, M. Watanabe, N. Kim, Y. Shiota, M. Koinuma, S. Takenaka, T. Sakai, E. Ertekin, T. Ishihara, A Cocatalyst That Stabilizes a Hydride Intermediate During Photocatalytic Hydrogen Evolution over a Rhodium- Doped TiO_2 Nanosheet. *Angew. Chem. Int. Ed.* **2018**, *57*, 9073-9077.

30. Han, S. W.; Hwang, Y. H.; Kim, S. H.; Yun, W. S.; Lee, J. D.; Park, M. G.; Ryu, S.; Park, J. S.; Yoo, D. H.; Yoon, S. P.; Hong, S. C.; Kim, K. S.; Park, Y. S. Controlling Ferromagnetic Easy Axis in a Layered MoS_2 Single Crystal. *Phys. Rev. Lett.* **2013**, *110*, 247201.